# Effects of In-Plane Load on Nonlinear Panel Flutter by Incremental Harmonic Balance Method

S. W. Yuen* and S. L. Lau†
*Hong Kong Polytechnic, Hung Hom, Hong Kong*

**The dynamical behavior of a hinged-hinged two-dimensional plate excited by supersonic flow is presented in this paper. The geometrical nonlinearity is considered using the large deflection plate theory, whereas the supersonic piston theory is employed to account for the effects of the aerodynamic force. A four-mode expansion has been used to reduce the original partial differential equation into a set of ordinary differential equations, which is then solved by the incremental harmonic balance method. In this study, the effects of the in-plane load are emphasized on the fluttering plate problem. The solution diagrams show that for a moderately high post-buckling load, several limit cycle oscillations are possible which have not yet been found beforehand. In addition, comparison of numerical results with other articles are made whenever data are available.**

## Nomenclature

$\boldsymbol{A}_0$ = matrix defined in Eq. (35)
$\Delta\boldsymbol{A}$ = matrix defined in Eq. (36)
$a_{in}$ = Fourier coefficients
$b$ = panel width $>> h$
$\boldsymbol{B}_{ij}$ = elements defined in Eq. (11)
$b_{im}$ = Fourier coefficients
$D$ = panel stiffness
$\boldsymbol{D}_{ij}$ = elements defined in Eq. (21)
$E$ = modulus of elasticity
$\boldsymbol{G}_i$ = elements defined in Eq. (23)
$\boldsymbol{g}$ = matrix defined in Eq. (44)
$h$ = panel thickness
$\boldsymbol{K}_j$ = elements defined in Eq. (10)
$\boldsymbol{k}$ = stiffness matrix defined in Eq. (41)
$l$ = panel length
$\boldsymbol{L}_{ij}$ = elements defined in Eq. (20)
$M$ = Mach number
$N_x$ = in-plane force ($x$-direction) induced by deflection
$N'_x$ = initial in-plane force ($x$-direction)
$N_{imkj}$ = elements defined in Eq. (12)
$n$ = mode number
$p$ = aerodynamic (perturbation) pressure
$Q_i$ = elements defined in Eq. (22)
$\boldsymbol{q}$ = matrix defined in Eq. (43)
$\boldsymbol{R}_i$ = elements defined in Eq. (24)
$\boldsymbol{r}$ = residual matrix defined in Eq. (42)
$R_x$ = $N'_x l^2/D$
$t$ = time
$U$ = wind velocity at infinity
$u$ = in-plane displacement
$\delta u$ = virtual in-plane displacement
$w$ = panel deflection
$\delta w$ = virtual panel deflection
$W$ = $w/h$
$\delta W$ = $\delta w/h$
$x$ = streamwise coordinate
$x_i$ = dependent variables
$\Delta x_i$ = increment of variable of $x_i$
$\boldsymbol{X}_0$ = matrix defined in Eq. (19)
$\Delta\boldsymbol{X}$ = matrix defined in Eq. (18)
$y$ = spanwise coordinate
$\rho_m$ = panel density
$\rho$ = air density
$\omega$ = oscillatory frequency
$\omega_L$ = $(D/\rho_m h l^4)^{1/2}$
$\beta$ = $\sqrt{M^2 - 1}$
$\tau$ = $\omega t$, nondimensionalized time
$\varepsilon$ = axial strain of panel
$\psi$ = curvature of panel
$\alpha$ = $x/l$
$\mu$ = $\rho l/\rho_m h$
$\lambda$ = $\rho U^2 l^3/\beta D$
$\nu$ = 0.3, Poisson's ratio
$\phi_i$ = $i$th linear mode shape
$\xi_i$ = $i$th modal amplitude (nondimensional)
$\delta\xi_i$ = $i$th virtual modal amplitude (nondimensional)

*Subscripts*
0 = current solution
$p$ = peak value

## I. Introduction

WHEN a plate or shell is exposed to an airflow along its surface, a self-excited oscillation may occur. This dynamic phenomenon is known as the *panel flutter*. Neglecting the structural nonlinearities, linear theory, which is commonly used in the classical analysis, indicates that there is a critical dynamic pressure (or flow speed) above which the panel motion becomes unstable and grows exponentially with time. This theory gives no information about the flutter oscillation itself except the flutter boundary and corresponding frequency. In fact, when the amplitude of the vibrations becomes large, to some extent, the effect of the in-plane stretching forces will be significant. These forces will restrain the plate motion so that only bounded limit cycle oscillations can be observed. The amplitude of vibrations, in general, grows as the dynamic pressure increases. An excellent survey on both linear and nonlinear panel flutter is given by Dowell.[1]

Various analytical techniques have been used to study nonlinear flutter behavior. Sarma and Varadan,[2] Mei,[3] and Mei and Rogers[4] analyzed the problem using the finite element method. In these studies, only a single assumed time mode was adopted. The Galerkin method, together with the assumed modes, is available to perform the same analysis. By this, the original partial differential equation is reduced to a

Received Aug. 15, 1990; revision received Feb. 11, 1991; accepted for publication Feb. 26, 1991. 

*Research Student, Department of Civil and Structural Engineering.
†Senior Lecturer, Department of Civil and Structural Engineering.

system of nonlinear ordinary differential equations. Many methods have been used to solve this system of equations. Dowell[5,6] employed the direct numerical integration and obtained valuable results. Evensen and Olson,[7] Kuo and Morino,[8] and Bolotin[9] used the harmonic balance method with single harmonic term to solve the equations, whereas the perturbation methods have also been used by Kuo and Morino[8] for the same problem.

In the present work, a two-dimensional hinged-hinged thin plate with geometrical nonlinearity under the action of an aerodynamic force is considered. The force is formulated using linear aerodynamic theory (appropriate to high supersonic Mach numbers). As the axial inertia is neglected and the supports are immovable, the nonlinear axial force (due to the deflection) must be constant over the whole length of the plate. By using a modal expansion, the governing partial differential equation is reduced to a system of ordinary differential equations. A six-mode expansion was recommended by Dowell.[5] However, after carrying out a rigorous analysis to determine the optimum number of modes that should be used in such kind of analyses (as many as 20 modes were studied), Dowell[6] concluded that a four-mode expansion was normally adequate to obtain satisfactory results. Therefore, a four-mode expansion has been adopted in the present work. The resulting system of equations can be solved by using the incremental harmonic balance (IHB) method and both stable and unstable solutions can be sought directly.

The IHB method does not make the assumption of small parameters and is capable of treating strongly nonlinear systems. It was originally presented for analyzing periodic structural vibrations by Lau and Cheung[10] and has been successfully applied to various types of nonlinear dynamic problems. For example, it was extended to treat dynamic instability of nonlinear structural systems by Lau et al.[11] and Pierre and Dowell[12]; it is also used in dry friction damper problems by Pierre, et al.[13] With the solution expanded into a multiple Fourier series containing a number of frequencies which are incommensurable with each other, the IHB method is also capable of treating aperiodic structural vibrations by Lau et al.[14] Recently, Lau and Zhang[15] have further generalized this method to deal with piecewise linear system problems.

The IHB method with a variable parameter is ideally suited to parametric studies for obtaining solution diagrams and is therefore used in the present studies. After obtaining the solution of a particular value of the parameter, this parameter will then be incremented. The new solution may be sought again by iterations using the previous solution as an approximation. By this means, solution diagrams of a dynamic system can easily be traced. To be more effective, Lau et al.[16] proposed an arc-length extrapolation procedure which can predict the neighboring state from some known states so that the required number of iterations to coverage can be reduced. The stability of the computed solution are readily analyzed by the use of the Floquet theory with Hsu's scheme, which was proposed by Friedmann et al.[17]

In this paper, the effects of the in-plane load on the fluttering plate are studied. The results of numerical solutions are presented and comparison are made to the available results wherever possible. The present results show a good agreement in most cases and new limit cycles are discovered.

## II. Problem Formulation and Solution Technique

By the virtual work equation on a largely deflected panel (Fig. 1) subjected to cylindrical bending, we obtain

$$\int_0^{2\pi}\int_0^{l} [D\psi\,\delta\psi + (N_x' + N_x)\,\delta\varepsilon + \rho_m h\,\ddot{w}\,\delta w]\,dx\,d\tau = \int_0^{2\pi}\int_0^{l} p\,\delta w\,dx\,d\tau \qquad (1)$$

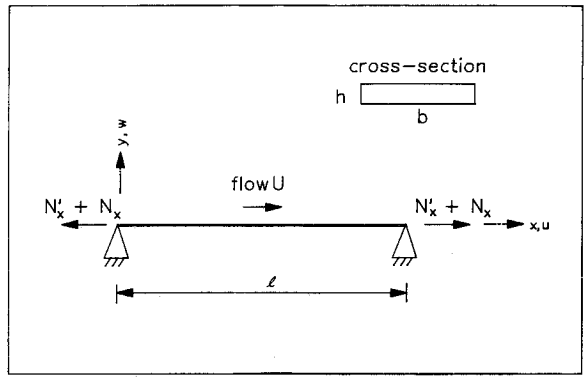


**Fig. 1 Panel geometry.**

where

$$\varepsilon = \frac{\partial u}{\partial x} + \frac{1}{2}\left(\frac{\partial w}{\partial x}\right)^2 \qquad \psi = \frac{\partial^2 w}{\partial x^2}$$

$$D = \frac{Eh^3}{12(1-\nu^2)} \qquad \tau = \omega t$$

where $(\dot{})$ denotes differential with respect to the dimensionless time variable $\tau$. In Eq. (1), the nonlinear term of $1/2(\partial w/\partial x)^2$ is added to approximate $\varepsilon$ in order to account for the effect of the axial force when the deflection of the panel is sufficiently large. The in-plane axial force $N_n$ can be regarded as constant over the whole length of the plate by neglecting the in-plane inertia; as the hinged-hinged plate is considered, $N_x$ is given by,

$$N_x = \frac{Eh}{2l}\int_0^{l}\left(\frac{\partial w}{\partial x}\right)^2 dx \qquad (2)$$

Assuming the aerodynamic pressure to be expressed by supersonic piston theory:

$$p = \frac{\rho U^2}{2\beta}\left[\frac{\partial w}{\partial x} + \left(\frac{M^2-2}{M^2-1}\right)\frac{\omega}{U}\frac{\partial w}{\partial \tau}\right] \qquad (3)$$

For $M \gg 1$,

$$\left(\frac{M^2-2}{M^2-1}\right)^2 \frac{\mu}{\beta} \text{ tends to } \frac{\mu}{M}$$

Nondimensionalizing Eqs. (1–3) gives

$$\int_0^{2\pi}\int_0^{1}\left\{\frac{\partial^2 W}{\partial\alpha^2}\cdot\frac{\partial^2\delta W}{\partial\alpha^2} + 6(1-\nu^2)\left[\int_0^{1}\left(\frac{\partial W}{\partial\alpha}\right)^2 d\alpha\right]\cdot\frac{\partial W}{\partial\alpha}\frac{\partial\delta W}{\partial\alpha} + R_x\frac{\partial W}{\partial\alpha}\cdot\frac{\partial\delta W}{\partial\alpha} + \left(\frac{\omega}{\omega_L}\right)^2\frac{\partial^2 W}{\partial\tau^2}\delta W + \lambda\left[\frac{\partial W}{\partial\alpha} + \frac{\omega}{\omega_L}\left(\frac{\mu}{M\lambda}\right)^{1/2}\frac{\partial W}{\partial r}\right]\delta W\right\} d\alpha\,d\tau = 0$$

for $M \gg 1$ (4)

where

$$W = \frac{w}{h} \qquad \alpha = \frac{x}{l} \qquad R_x = \frac{N_x' l}{D}$$

$$\mu = \frac{\rho l}{\rho_m h} \qquad \lambda = \frac{\rho U^2 l^3}{\beta D} \qquad \omega_L^2 = \frac{D}{\rho_m h l^4}$$

### A. Modal Expansion

According to Galerkin's method, the transverse deflection $W$ can be approximated using a series of mode shapes $\phi_i(\alpha)$ as

$$W(\alpha,\tau) = \sum_{i=1}^{n} \phi_1(\alpha)\, \xi_i(\tau) \tag{5}$$

where $n = 4$ for the present analysis. Similarly, the variation with respect to the coordinates $\xi_i$ reads

$$\delta W(\alpha,\tau) = \sum_{j=1}^{n} \phi_j(\alpha)\, \delta\xi_j \tag{6}$$

For a hinged-hinged plate, the linear mode shapes are given by

$$\phi_j(\alpha) = \sin j\pi\alpha \qquad j = 1, \ldots, 4 \tag{7}$$

After substituting Eq. (5) and Eq. (6) into Eq. (4), and performing the integration with respect to $\alpha$ regarding the orthogonal properties of the linear mode shapes, we can get an equivalent set of differential equations:

$$\left(\frac{\omega}{\omega_L}\right)^2 \xi_j + C\left(\frac{\omega}{\omega_L}\right)\lambda^{1/2}\,\dot{\xi}_j + \boldsymbol{K}_j\xi_j + \lambda \sum_{I=1}^{n} \boldsymbol{B}_{ij}\xi_i + \sum_{i}^{n}\sum_{m}^{n}\sum_{k}^{n} \boldsymbol{N}_{imkj}\xi_i\xi_m\xi_k = 0 \qquad j = 1, \ldots, 4 \tag{8}$$

where

$$C = \frac{\mu}{M} \tag{9}$$

$$\boldsymbol{K}_j = \frac{1}{\boldsymbol{F}_i}\left\{\int_0^1 \phi_j''\, d\alpha + R_x \int_0^1 \phi_j'^2\, d\alpha\right\} \tag{10}$$

$$\boldsymbol{B}_{ij} = \frac{1}{\boldsymbol{F}_j}\left\{\int_0^1 \phi_j'\phi_j\, d\alpha\right\} \tag{11}$$

$$\boldsymbol{N}_{imkj} = \frac{6(1-\nu^2)}{\boldsymbol{F}_j}\left\{\int_0^1 \phi_i'\phi_j'\, d\alpha\right\}\left\{\int_0^1 \phi_m'\,\phi_k\, d\alpha\right\} \tag{12}$$

in which

$$\boldsymbol{F}_j = \int_0^1 \phi_j^2\, d\alpha \tag{13}$$

Here, (′) denotes differentiation with respect to $\alpha$.

### B. IHB Formulation

Eq. (8) can generally be expressed as a system of nondimensional simultaneous equations as follows:

$$\omega^2\ddot{x}_i + f_i(x_1, \ldots, x_n, \dot{x}_1, \ldots, \dot{x}_n, \omega, \lambda) = 0 \qquad i = 1, \ldots, n \tag{14}$$

where a dot denotes differentiation with respect to the dimensionless time $\tau$, and $f_i(x_1, \ldots, x_n, \dot{x}_1, \ldots, \dot{x}_n, \omega, \lambda)$ is a nonlinear function of the dimensionless oscillation frequency $\omega$, the parameter $\lambda$, the dependent variable $x_i$, and its velocity $\dot{x}_i$.

The procedure of the IHB method for seeking periodic solutions is mainly divided into two steps. In the first step, small increments (symbolized by $\Delta$) are added to the current solution (or a guessed solution at the beginning of the procedure) of Eq. (14), i.e., $\omega_0$, $\lambda_0$, and $x_{i0}$ $(i = 1,2, \ldots, n)$ to get a neighboring solution:

$$\omega = \omega_0 + \Delta\omega$$
$$\lambda = \lambda_0 + \Delta\lambda$$
$$x_i = x_{i0} + \Delta x_i \qquad i = 1, \ldots, n \tag{15}$$

Expanding Eq. (14) by Taylor's series about the initial state and neglecting all the nonlinear terms of small increments will yield the linearized incremental equation:

$$\omega_0^2\,\Delta\ddot{x}_i + \sum_{j=1}^{n}\left(\frac{\partial f_i}{\partial \dot{x}_j}\right)_0 \Delta\dot{x}_j + \sum_{j=1}^{n}\left(\frac{\partial f_i}{\partial x_j}\right)_0 \Delta x_j = -(\omega_0^2\ddot{x}_{i0} + f_{i0}) - \left[\left(\frac{\partial f_i}{\partial \omega}\right)_0 + 2\omega_0\ddot{x}_{0i}\right]\Delta\omega - \left(\frac{\partial f_i}{\partial \gamma}\right)_0 \Delta\lambda \qquad i = 1,2, \ldots, n \tag{16}$$

This variational equation is equivalent to the linear matrix equation for the increments

$$\omega^2\Delta\ddot{\boldsymbol{X}} + \boldsymbol{D}\cdot\Delta\dot{\boldsymbol{X}} + \boldsymbol{L}\cdot\Delta\boldsymbol{X} = \boldsymbol{R} - (2\omega\cdot\ddot{\boldsymbol{X}}_0 + \boldsymbol{Q})\cdot\Delta\omega - \boldsymbol{G}\cdot\Delta\lambda \tag{17}$$

where

$$\Delta\boldsymbol{X} = [\Delta x_1, \Delta x_2, \ldots, \Delta x_n]^T \tag{18}$$

$$\boldsymbol{X}_0 = [x_{10}, x_{20}, \ldots, x_{n0}]^T \tag{19}$$

The elements of the matrices $\boldsymbol{L}$ and $\boldsymbol{D}$ are given by

$$\boldsymbol{L}_{ij} = \left(\frac{\partial f_i}{\partial x_j}\right)_0 \tag{20}$$

$$\boldsymbol{D}_{ij} = \left(\frac{\partial f_i}{\partial \dot{x}_j}\right)_0 \tag{21}$$

and the elements of the vectors $\boldsymbol{Q}$, $\boldsymbol{G}$, and $\boldsymbol{R}$ are

$$\boldsymbol{Q}_i = \left(\frac{\partial f_i}{\partial \omega}\right)_0 \tag{22}$$

$$\boldsymbol{G}_i = \left(\frac{\partial f_i}{\partial \gamma}\right)_0 \tag{23}$$

$$\boldsymbol{R}_i = -[\omega_0^2\ddot{x}_{i0} + f_{i0}] \tag{24}$$

In Eq. (17), $\boldsymbol{R}$ is a corrective term to prevent the incrementation process drifting away from the actual solution.

The second step of the IHB method is the Galerkin procedure, namely, performing the integration with respect to $\tau$ in Eq. (4). Assume that the unknown $x_0$ can be expanded into a truncated Fourier series:

$$x_{i0} = \sum_{n=n1,n2,\ldots} a_{in}\cos n\tau + \sum_{m=m1,m2,\ldots} b_{im}\sin m\tau \qquad i = 1, \ldots, n \tag{25}$$

where the progressions $n_1, n_2, \ldots$ and $m_1, m_2, \ldots$ are positive integers. They may be 0, 1, 2, . . . or 1, 3, 5, . . . etc, subject to the circumstance.

Similarly, $\Delta x$ is expanded as

$$\Delta x_i = \sum_{n\ n1,n2,\ldots} \Delta a_{in}\cos n\tau + \sum_{m\ m1,m2,\ldots} \Delta b_{im}\sin m\tau \qquad i = 1, \ldots, n \tag{26}$$

For conciseness, the functions $x_0$ and $\Delta x$ can be rewritten as

$$x_{i0} = \boldsymbol{T}\,\boldsymbol{a}_{i0} \tag{27}$$

$$\Delta x_i = \boldsymbol{T}\,\Delta a_i \qquad i = 1, \ldots, n \tag{28}$$

where

$$\boldsymbol{T} = [\cos n_1\tau, \cos n_2\tau_1, \ldots, \sin m_1\tau, \sin m_2\tau, \ldots] \quad (29)$$

$$\boldsymbol{a}_{i0} = [a^0_{in_1}, a^0_{in_2}, \ldots, b^0_{im_1}, b^0_{im_2}, \ldots]^T \quad i = 1, \ldots, n \quad (30)$$

$$\Delta\boldsymbol{a}_i = [\Delta a_{in_1}, \Delta a_{in_2}, \ldots, \Delta b_{im_1}, \Delta b_{im_2}, \ldots]^T \quad i = 1, \ldots, n \quad (31)$$

Therefore,

$$\boldsymbol{X}_0 = \boldsymbol{Y}\cdot\boldsymbol{A}_0 \quad (32)$$

$$\Delta\boldsymbol{X} = \boldsymbol{Y}\cdot\Delta\boldsymbol{A} \quad (33)$$

where

$$\boldsymbol{Y} = \begin{bmatrix} \boldsymbol{T} & & 0 \\ & \boldsymbol{T} & \\ & & \ddots \\ 0 & & \boldsymbol{T} \end{bmatrix} \quad (34)$$

$$\boldsymbol{A}_0 = [\boldsymbol{a}^T_{10}, \boldsymbol{a}^T_{20}, \ldots, \boldsymbol{a}^T_{n0}]^T \quad (35)$$

$$\Delta\boldsymbol{A} = [\Delta\boldsymbol{a}^T_1, \Delta\boldsymbol{a}^T_2, \ldots, \Delta\boldsymbol{a}^T_n]^T \quad (36)$$

With these notations, we have

$$\dot{\boldsymbol{X}}_0 = \dot{\boldsymbol{Y}}\,\boldsymbol{A}_0 \quad (37)$$

$$\ddot{\boldsymbol{X}}_0 = \ddot{\boldsymbol{Y}}\,\boldsymbol{A}_0 \quad (38)$$

By substituting Eqs. (32), (33), (37), and (38) into Eq. (17), and applying the Galerkin procedure for one period, we obtain

$$\delta\Delta\boldsymbol{A}^T \left\{ \int_0^{2\pi} \boldsymbol{Y}^T [\omega_0^2\,\ddot{\boldsymbol{Y}} + \boldsymbol{D}\cdot\dot{\boldsymbol{Y}} + \boldsymbol{L}\cdot\boldsymbol{Y}]\,d\tau \right\} \Delta\boldsymbol{A} = \delta\Delta\boldsymbol{A}^T \left\{ \int_0^{2\pi} \boldsymbol{Y}^T\cdot\boldsymbol{R}\,d\tau - \int_0^{2\pi} \boldsymbol{Y}^T \cdot[\boldsymbol{Q} + 2\omega_0\ddot{\boldsymbol{Y}}\cdot\boldsymbol{A}_0]\,d\tau\,\Delta\omega - \int_0^{2\pi} \boldsymbol{Y}^T\cdot\boldsymbol{G}\,d\tau\cdot\Delta\gamma \right\} \quad (39)$$

Or simply,

$$\boldsymbol{k}\,\Delta\boldsymbol{A} = \boldsymbol{r} + \boldsymbol{q}\,\Delta\omega + \boldsymbol{g}\,\Delta\lambda \quad (40)$$

where the matrix

$$\boldsymbol{k} = \int_0^{2\pi} \boldsymbol{Y}^T [\omega_0^2\,\ddot{\boldsymbol{Y}} + \boldsymbol{D}\cdot\dot{\boldsymbol{Y}} + \boldsymbol{L}\cdot\boldsymbol{Y}]\,d\tau \quad (41)$$

and the vectors

$$\boldsymbol{r} = \int_0^{2\pi} [\omega_0^2\,\dot{\boldsymbol{Y}}^T\cdot\dot{\boldsymbol{Y}}\cdot\boldsymbol{A}_0 - \boldsymbol{Y}^T\cdot\boldsymbol{F}_0]\,d\tau \quad (42)$$

$$\boldsymbol{q} = \int_0^{2\pi} [2\omega_0\dot{\boldsymbol{Y}}^T\dot{\boldsymbol{Y}}\,\boldsymbol{A}_0 - \boldsymbol{Y}^T\boldsymbol{Q}]\,d\tau \quad (43)$$

$$\boldsymbol{g} = -\int_0^{2\pi} \boldsymbol{Y}^T\,\boldsymbol{G}\,d\tau \quad (44)$$

Refer to Eq. (40), the number of unknowns is more than that of equation by two; they are the frequency of the limit cycle $\omega$ and the parameter $\lambda$. As far as only the limit cycle is concerned, $\lambda$ is taken to be the control parameter (i.e., $\Delta\lambda$ is given), while $\Delta\omega$ should be regarded as an unknown. Therefore, one of the Fourier coefficient has to be fixed (e.g., $a_{i1} = 0$ or $b_{i1} = 0$) to make the number of equations equal to that of the unknowns. It will not cause any effects because this system is autonomous and indeed it only represents a shift of response on the time axis.

With the column corresponding to coefficient $b_{i1}$ say, replaced by $\boldsymbol{q}$ in $\boldsymbol{k}$ and $\Delta b_1$ replaced by $\Delta\omega$, we have

$$\boldsymbol{k}'\,\Delta\boldsymbol{A}' = \boldsymbol{r} \quad (45)$$

where $\boldsymbol{k}'$ and $\Delta\boldsymbol{A}'$ are the corresponding matrix $\boldsymbol{k}$ and vector $\Delta\boldsymbol{A}$ after such replacement, respectively. Eq. (45) can be solved by any equation solver. A better approximation can be obtained by iterations. The iteration process is then carried out with updated $\boldsymbol{k}'$ and $\boldsymbol{r}$ each time until a certain allowance is reached.

After obtaining solution for a particular $\lambda$, it is then added by an increment, $\Delta\lambda$ (known as the control increment). This is known as an augmentation process. The iteration process is repeated again using the previous solution as an approximation until the solution for the neighboring $\lambda$ is sought. By this means, the neighboring solution can also be sought. By successive use of augmentation and iteration process, a solution diagram may easily be traced. Alternatively, the frequency $\omega$, or one of the Fourier coefficients $a_{ij}$ and $b_{ij}$ may also be used as the control increment in the above augmentation process. The choice of the control increment depends on the rate of the variation of the increments; usually the one with the greatest increment (absolute values) will be chosen as the control increment. This is extremely useful when a solution diagram is very sensitive to the variation of the parameter $\lambda$ or the like. The number of the steps to trace the solution diagram will be reduced.

As the IHB formulation follows the Newton-Raphson procedure, the magnitude of the control increment is chosen so as to reduce the number of iterations. Normally, a finite number of iterations (four iterations, say) is deemed to be adequate for the calculation. With this criterion, the magnitude of the control increment will be controlled by the shape of the curve in a solution diagram being traced.

To be more efficient, an incremental arc-length extrapolation method can be used to predict the next solution. The number of iterations required for convergent solution will be greatly reduced. Further, it is also useful in handling the convergence problem at peaks of the solution curves. A solution diagram for the parametric study can be obtained by computer with this technique and the IHB method installed in the same program.

## III. Results

It is of great interest to study the effects of the in-plane loading on a fluttering plate. Dowell[5,6,18] has obtained interesting and valuable results by applying the time integration to a similar model. Complicated motions will occur when a fluid flow over the upper surface of the plate under a compressive in-plane load ($R_x$ is negative). In this study, it is discovered that when $R_x \le -2\pi^2$, several limit cycle vibrations are feasible for a given value of dynamic pressure $\lambda$. Some of them are stable, whereas some are not. The extraperiodic motions can only be sought with the presence of higher harmonic terms. On the other hand, chaos and aperiodic motions are reported by Dowell.[5,6,18]

To be comparable to the results computed by Dowell[5,6,18] and Kuo and Morino,[8] the amplitude of $w/h$ (peak values of the panel response in the time history, denoted by $(w/h)_p$) at $x/l = 0.75$ will be plotted against the parameter $\lambda$. Further, $\mu/M = 0.01$ is assumed unless otherwise stated and periodic solutions are main objectives to be discussed.

### A. $R_x = -2\pi^2$

The first case being examined is $R_x = -2\cdot\pi^2$. $(w/h)_p$ is plotted against $\lambda$, as shown in Fig. 2. The IHB results are compared with those computed by Dowell[5] using the numerical integration (NI) method and Kuo and Morino[8] using the harmonic balance (HB) method.

In the IHB calculation, if a single assumed time mode (cos $\tau$ and sin $\tau$) is used, the HB method (denoted by $\Delta$) and IHB method (dashed line) give the same results as expected. This can be seen from Fig. 2, where the symbols $\Delta$ lie on the dashed line (curve 2). However, if four odd harmonic terms ($\cos\tau$, $\cos3\tau$, . . . , $\cos7\tau$, $\sin\tau$, $\sin3\tau$, . . . , $\sin7\tau$) are used in the IHB calculation, the result indicated by curve 1 is shown on the right-hand side of the figure. The outbursts of a loop of curve is a main difference between the present analysis and that by Kuo and Morino.[8] This loop cannot be seen if the higher harmonics ($3\tau$, $5\tau$, and $7\tau$) are not used as they are dominant components of the vibration. To guarantee the sufficient number of harmonic terms have been used, as many as seven odd harmonic terms are used to carryout the analysis. It is found that four odd harmonic terms are adequate for the present calculation.

Dowell[5,8] calculated the panel flutter problems by the NI method and provided accurate results; however, the solution diagram had not yet been completed; more or less, the result is similar to that calculated by Kuo and Morino.[8] From Fig. 2, three limit cycles of different amplitudes can be found for a particular $\lambda$ within the range between 323.0 and 396.0. Two more solutions (one stable plus one unstable) are in fact missing for $\lambda$ on this interval. A limit cycle motion does not depend on the initial conditions (a steady state will be reached after a transient state), but which motion of the three limit cycles will actually happen? The answer for this will depend on which basin the starting point is; the subsequent motion will then approach this particular limit cycle (if it is stable).

Equilibrium states (curve 2) can be found on the left-hand side of Fig. 2. These curves illustrate that the panel is buckled but dynamically stable, which coincides with that obtained by Dowell.[6] Five harmonic terms ($\cos0\tau$, $\cos2\tau$, . . . , $\cos4\tau$, $\sin\tau$, $\sin2\tau$, . . . , $\sin4\tau$) are sufficient to obtain satisfactory results.

### B. $R_x = -3\pi^2$

Next, the case for $R_x = -3\cdot\pi^2$ is considered. The solution diagram by the IHB method ($(w/h)_p$ versus $\lambda$) is presented in Fig. 3. The same number of harmonics is employed as in the previous case. This diagram is quite similar to the case $R_x = -2\cdot\pi^2$ except that the loop occurs at $350.0 < \lambda < 424.0$. Instead of plotting the amplitude of vibration against $\lambda$, the diagram of the frequency $\omega$ verse $\lambda$ may also provide interesting information (Fig. 4). Limit cycles for $\lambda = 372.9$ are given in Fig. 5.

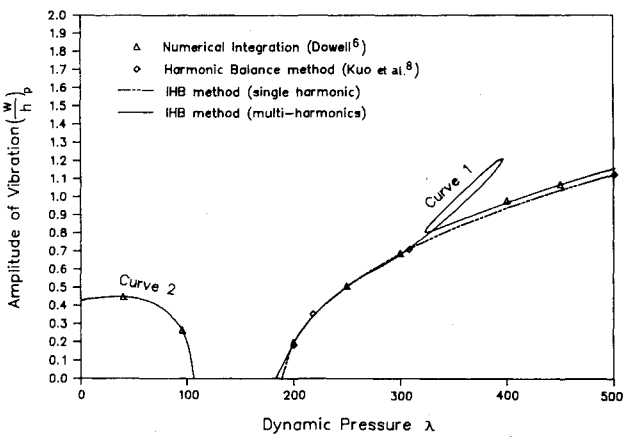


Fig. 2 Amplitude against dynamic pressure ($R_x = -2\pi^2$).

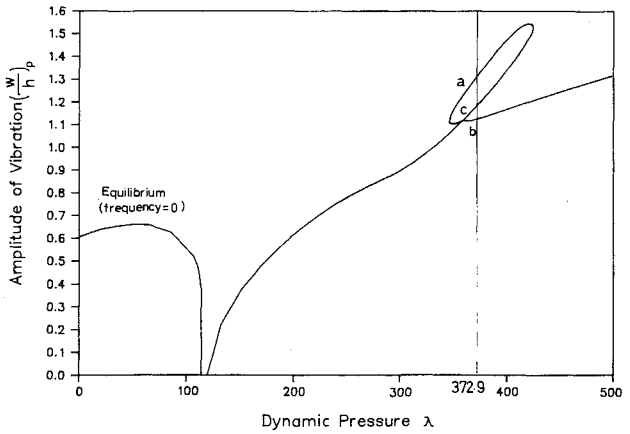


Fig. 3 Amplitude against dynamic pressure ($R_x = -3\pi^2$).

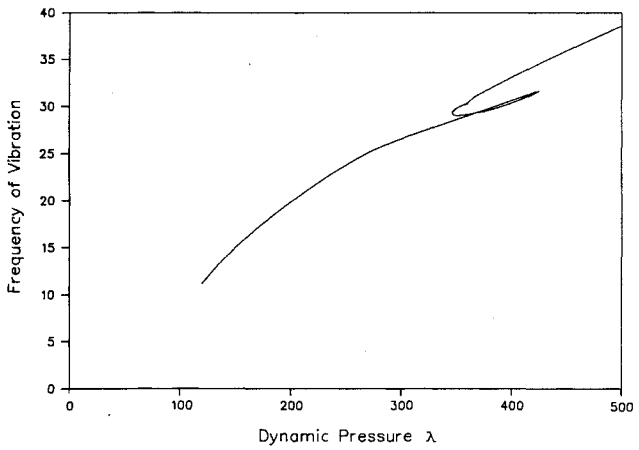


Fig. 4 Frequency against dynamic pressure ($R_x = -3\pi^2$).

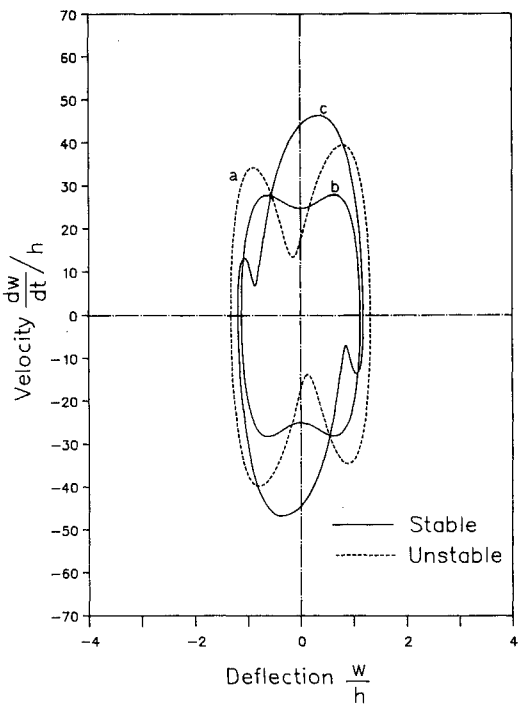


Fig. 5 Limit cycle by IHB method ($\lambda = 372.9$, $R = -3\pi^2$).

To have a clear understanding of the limit cycle motion, the motions of the plate over a half-period of oscillation for $\lambda = 372.9$, $R_x = -3\pi^2$ are illustrated in Figs 6a–6c. The second half-period motions are just the mirror images of the shown ones. Both motions shown in Fig. 6b and Fig. 6c are stable while that shown in Fig. 6a is unstable.

Although attention is drawn on periodic solutions, nonperiodic solutions also exist. The case $\lambda = 150.0$ is examined carefully with the program "Dynamic Software," using a standard numerical integration procedure. Apart from a stable solution, an extra solution is found and shown in Fig. 7a.

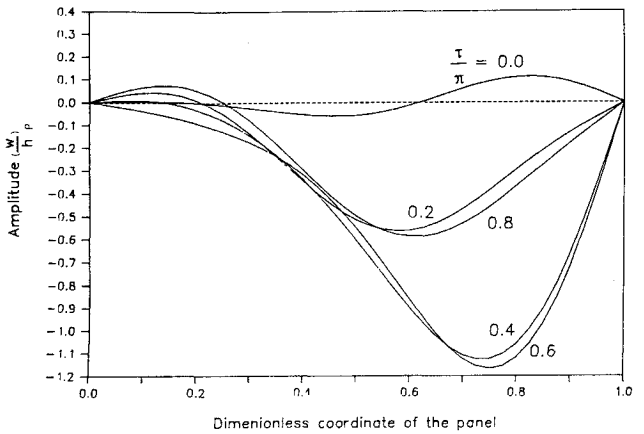


**a) $\lambda = 372.9$, $R_x = -3\pi^2$, and $\omega = 29.44$: unstable (limit cycle "a" in Fig. 5)**

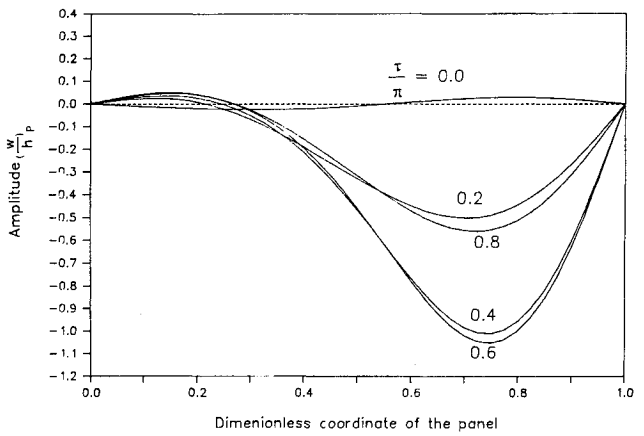


**b) $\lambda = 372.9$, $R_x = -3\pi^2$, and $\omega = 31.50$: stable (limit cycle "b" in Fig. 5)**

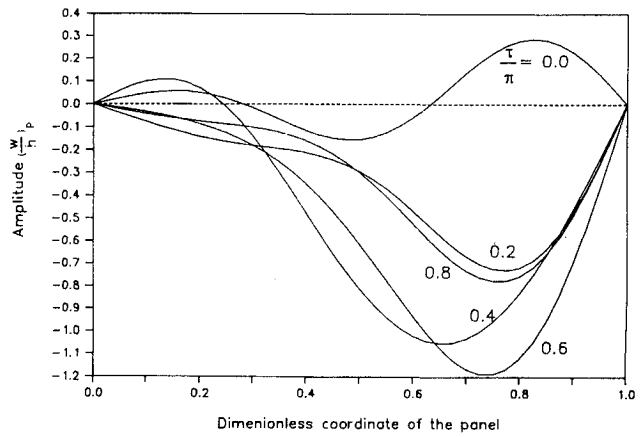


**c) $\lambda = 372.9$, $R_x = -3\pi^2$, and $\omega = 29.56$: stable (limit cycle "c" in Fig. 5)**

**Fig. 6 Half-period of limit cycle.**

The result is obtained after 20,000 convergent steps with time increment equal to 0.001. The solution seems to be periodic as only "one limit cycle" is obtained. After further investigation, nevertheless, it was found that the motion is nonperiodic. Being a blow-up picture of Fig. 7a, Fig. 7b shows that this "limit cycle" in fact consists of a number of lines that are different form one another. This contradicts the fact that a periodic solution gives exactly one trajectory after steady state has been touched. A similar observation was given by Dowell[6] for $\mu/M = 0.01$. Moreover, the IHB procedure cannot find out a convergent solution for this case, which further shows that this extra solution is not periodic and the possibility of numerical inaccuracy of the NI results will be very low.

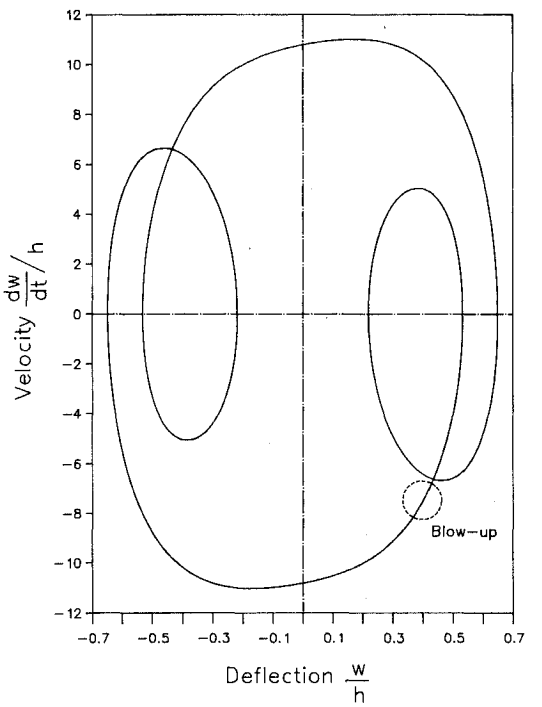


**Fig. 7a Limit cycles by the NI method with time step equal to 0.001 ($\lambda = 150.0$, $R_x = -3\pi^2$).**

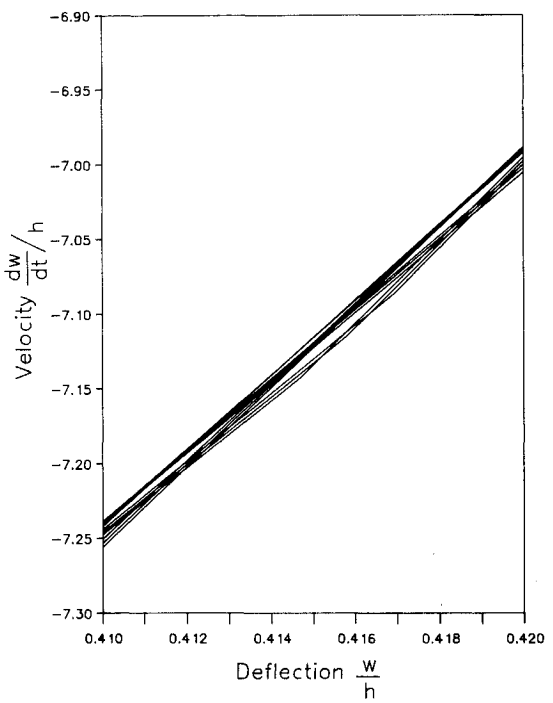


**Fig. 7b Blow-up of Fig. 7a.**

### C. $R_x = -4\pi^2$

Similar to the previous cases, the case for $R_x = -4 \cdot \pi^2$ is also computed. The diagram of $(w/h)_p$ vs $\lambda$ is shown in Fig. 8. With reference to Fig. 8, a loop occurs in the range $361.5 \leq \lambda \leq 476.9$. Limit cycle behavior for $\lambda = 377.3$ (Fig. 9) is found to exhibit a total of five limit cycles! Three of them are stable and the rest are unstable.

It should also be noted that another loop occurs around $\lambda = 200.0$ and a representative limit cycle ($\lambda = 201.40$) is given in Fig. 10. The motion tends to be unstable with decreasing value of $\lambda$ (Fig. 11). Finally, it becomes nonperiodic when $\lambda$ is less than about 170.0. In this situation, the NI method is the only way to compute the nonperiodic motions. A chaos was found and is shown in Fig. 12 ($\lambda = 150$). An intensive and heuristic explanation of the appearance of chaotic motion has been given by Dowell.[6]

## IV. Concluding Remarks

In this study, attention is focused on the effects of the in-plane loading on the limit cycle motion of a fluttering plate. In the examples provided, solution diagrams of the in-plane loads $R_x = -2 \cdot \pi^2$, $-3 \cdot \pi^2$, and $-4 \cdot \pi^2$ are calculated. In the plots of $(w/h)_p$ against $\lambda$, various loops are observed, which are the main discoveries of this study. These loops seem to have some intersecting points on the diagrams shown; in fact, these curves are nowhere intersecting if they are viewed in a multidimensional space formed by the Fourier amplitudes, frequency $\omega$, and parameter $\lambda$. There are as many as five limit cycles coexisting at a particular $\lambda$. With different starting points, the plate can vibrate at one of the limit cycle motions and the amplitude of flutter will depend on which limit cycle actually occurs.

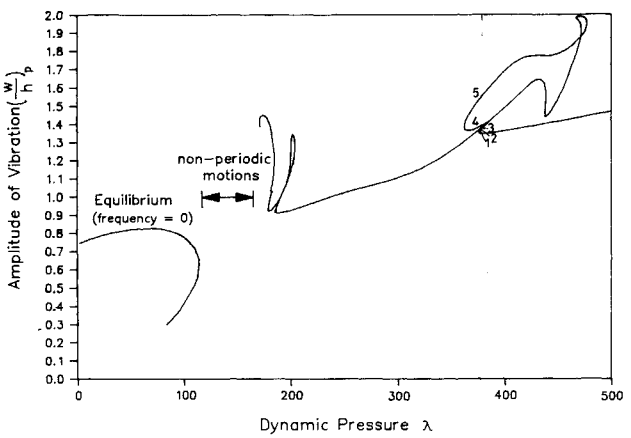


Fig. 8 Amplitude against dynamic pressure ($R_x = -4\pi^2$).

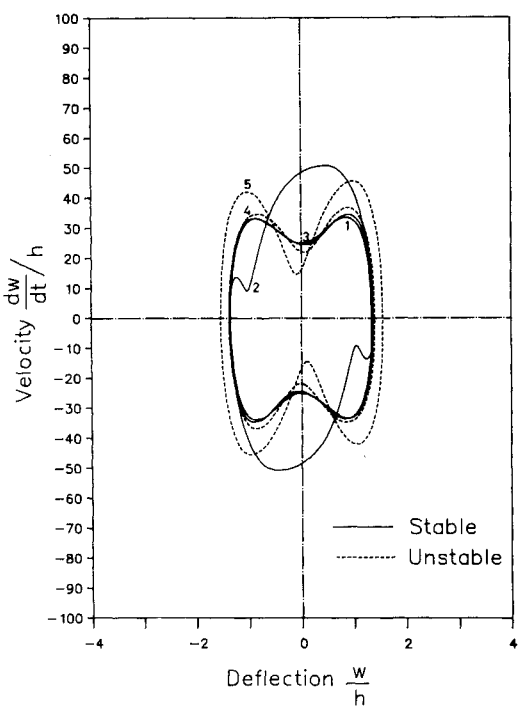


Fig. 9 Limit cycle by IHB method ($\lambda = 377.3$, $R_x = -4\pi^2$).

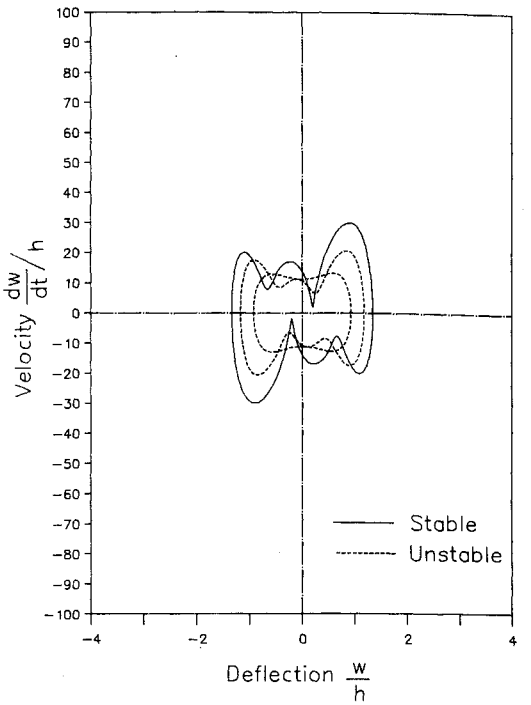


Fig. 10 Limit cycle by IHB method ($\lambda = 201.4$, $R_x = -4\pi^2$).

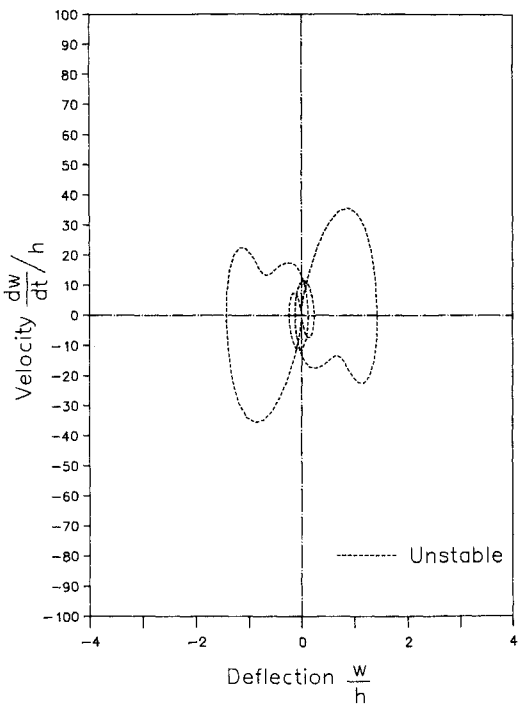


Fig. 11 Limit cycle by IHB method ($\lambda = 171.1$, $R_x = -4\pi^2$).

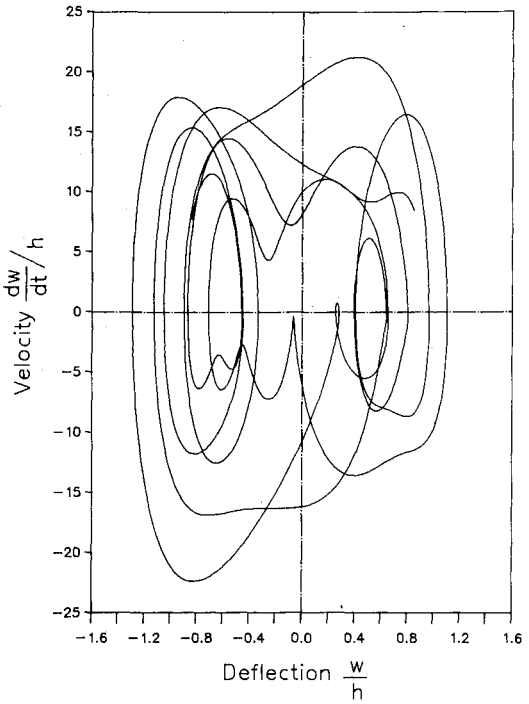


**Fig. 12 Trajectory by the NI method ($\lambda = 150.0$, $R_x = -4\pi^2$).**

The stabilities of the limit cycle motions are also important, which can be analyzed by the Floquet theory. Obviously, only the stable ones can exist in the physical world. Nevertheless, unstable periodic solutions are also important as the study of their birth and death will provide additional understanding and insight into the transition to chaos.

On the other hand, nonperiodic motions also occur for this problem of supersonic flow over the upper surface of a plate under a compressive in-plane load. These motions may be either chaotic or aperiodic. If a fluid flows at a sufficiently large velocity, the plate will flutter with a periodic harmonic motion if no compressive in-plane load exists. In between the said cases, the plate will undergo nonperiodic motions, as suggested by Dowell.[5,6,18] For example, a chaos occurs at $\mu/M = 0.01$, $R_x = -4\cdot\pi^2$, and $\lambda = 150.0$, as shown in Fig. 12. At $R_x = -3\cdot\pi^2$ and $\lambda = 150.0$, a nonperiodic solution is observed in Figs. 7a and 7b. The IHB method is not derived to seek chaotic solutions, but is capable of calculating an almost periodic one, as proposed by Lau.[14] The phenomenon of appearance of almost periodic motion has been the focus of recent research because of its wide applications to many dynamical systems. The authors recommend a further study on the almost periodic oscillation and its occurrence by the IHB method.

## References

[1]Dowell, E. H., "Panel Flutter: A Review of the Aeroelastic Stability of Plates and Shells," *AIAA Journal*, Vol. 8, No. 3, March 1970, pp. 385–399.

[2]Sarma, B. S., and Varadan, T. K., "Nonlinear Panel Flutter by Finite-Element Method," *AIAA Journal*, Vol. 26, No. 5, May 1988, pp. 566–574.

[3]Mei, C., "A Finite Element Approach for Nonlinear Panel Flutter," *AIAA Journal*, Vol. 15, No. 8, Aug. 1977, pp. 1107–1110.

[4]Mei, C., and Rogers, J. L., Jr., "NASTRAN-Nonlinear Vibration Analysis of Beams and Frame Structures," NASA TMX-3278, 1975, pp. 259–284.

[5]Dowell, E. H., "Nonlinear Oscillations of a Fluttering Plate," *AIAA Journal*, Vol. 4, No. 7, July, 1966, pp. 1267–1275.

[6]Dowell, E. H., "Flutter of a Buckled Plate as an Example of Chaotic Motion of a Deterministic Autonomous System," *Journal of Sound and Vibration*, Vol. 85, 1982, pp. 333–344.

[7]Evensen, D. A., and Olson, M. D., "Nonlinear Flutter of Circular Cylindrical Shell in Supersonic Flow," TND-4265, 1967.

[8]Kuo, C. C., and Morino, L., "Perturbation and Harmonic Balance Methods for the Nonlinear Panel Flutter," *AIAA Journal*, Vol. 10, No. 11, Nov. 1972, pp. 1479–1484.

[9]Bolotin, V. V., *Nonconservative Problems of the Theory of Stability*. Macmillan, New York, 1963, pp. 274–312.

[10]Lau, S. L., and Chueng, Y. K., "Amplitude Incremental Variational Principle for Nonlinear Vibration of Elastic System," *ASME Journal of Applied Mechanics*, Vol. 48, 1981, pp. 959–964.

[11]Lau, S. L., Cheung, Y. K., and Wu, S. Y., "A Variable Parameter Incrementation Method for Dynamic Instability of Linear and Nonlinear System," *ASME Journal of Applied Mechanics*, Vol. 49, 1982, pp. 849–853.

[12]Pierre, C., and Dowell, E. H., "A Study of Dynamic Instability of Plates by an Extended Incremental Harmonic Balance Method," *ASME Journal of Applied Mechanics*, Vol. 52, 1985, pp. 693–697.

[13]Pierre, C., Ferri, A. A., and Dowell, E. G., "Multi-harmonic Analysis of Dry Friction Damped Systems Using an Incremental Harmonic Balance Method," *ASME Journal of Applied Mechanics*, Vol. 52, 1985, pp. 658–694.

[14]Lau, S. L., Cheung, Y. K., and Wu, S. Y., "Incremental Harmonic Balance Method with Multiple Time Scales for Aperiodic Vibration of Nonlinear Systems," *ASME Journal of Applied Mechanics*, Vol. 50, 1983, pp. 871–876.

[15]Lau, S. L., and Zhang, W-S., "Nonlinear Vibrations of Piecewise-Linear Systems by Incremental Harmonic Balance Method," *ASME Journal of Applied Mechanics*, 1991, in press.

[16]Lau, S. L., Cheung, Y. K., and Wu, S. Y., "Nonlinear Vibration of Thin Elastic Plates Part II. Internal Resonance," *ASME Journal of Applied Mechanics*, Vol. 51, 1984, pp. 845–851.

[17]Friedmann, P., hammond, C. E., and Woo, T. H., "Efficient Numerical Treatment of Periodic Systems with Application to Stability Problems," *International Journal for Numerical Methods in Engineering*, Vol. 11, 1977, pp. 1117–1136.

[18]Dowell, E. H., "Observation and Evolution of Chaos for an Autonomous System," *ASME Journal of Applied Mechanics*, Vol. 51, 1984, p. 664–673.